Optimization of the shape of material for enhancing the power output of thermomagnetic oscillator

Shivam Shukla[1] and Deepak K[1,*]

[1] Department of Metallurgical Engineering, Indian Institute of Technology (BHU), Varanasi, UP, India
* Corresponding author email: deepak.met@iitbhu.ac.in

Abstract

The world's energy needs are substantially increasing day by day and shifting towards renewable resources for energy production.Waste heat is an inevitable and infelicitous product of a large number of industrial processes. The technologies that can convert waste heat into useful energy output are being explored in recent times. They are based on the functional response of materials such as, piezoelectric, thermoelectric, thermomagnetic, etc.

To utilize waste heat or low grade energy a Thermomagnetic Oscillator (TMO) was developed recently which was one the most effective way of utilizing waste heat. In this study, we had optimized the shape of thermomagnetic alloy in a such a way that induced voltage had increased by 152% just only upward motion of thermomagnetic alloy (TMA) in thermomagnetic oscillator. In this device, two opposite directional forces i.e. magnetic force of the magnet (F_m in upward direction) and gravitational force (F_g in downward direction) were applied on TMM for its oscillation. For optimizing the shape of TMM, we had used Eulerian approach of fluid flow to analyze the heating and cooling phenomena of TMM and found that induced voltage had increased up to 4.73V during only upward motion of thermomagnetic material.

Key words: Thermomagnetic oscillator (TMO), Magnetic Fields (mf) module, Energy Harvesting, Thermomagnetic material (TMM) and Waste heat utilization.

1. Introduction

A Thermomagnetic Oscillator was demonstrated recently [1] to extract electricity from waste heat. The schematic and the experimental setup of Thermomagnetic Oscillator (TMO) is shown in Fig. 1, which comprises of a cylindrical thermomagnetic alloy (TMA) that oscillates between the heat source and heat sink due to the temperature gradient and the magnetic force from a permanent magnet. The electricity was generated due to the oscillation of the thermomagnetic alloy.

The most important step that controls the frequency of this oscillator and power generation was the heat transfer between the heat load/sink and the thermomagnetic alloy [2].To achieve better power output, frequency of oscillation & induced voltage, a modification in the shape of the thermomagnetic material (TMM) inside the oscillator was done. There are multiple COMSOL models which deal with magnetic fields [3] [4] [5], electromagnetic induction [6][7], heat transfer [8][9]. By exploring these previous models and enhancing them to suit our functionality, three models for the thermomagnetic material in the shape of bulk cylinder, fins geometry & spiral geometry were built and simulated for heat transfer phenomena in heat transfer module in COMSOL (Fig. 2).

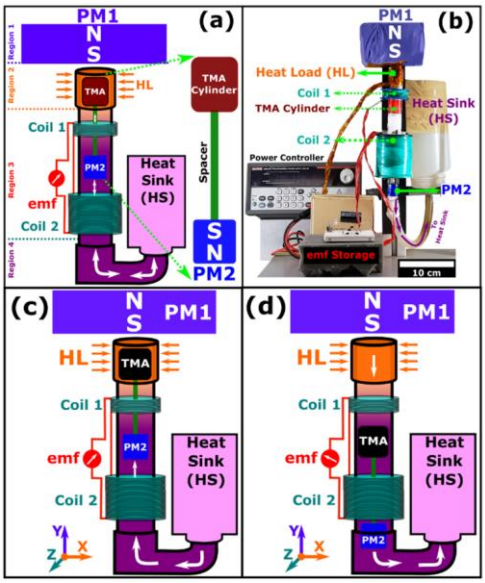

***Fig.1**: Schematic of TMO showing the heating and cooling cycles (a, b and d). Experimental setup (b)[1]*

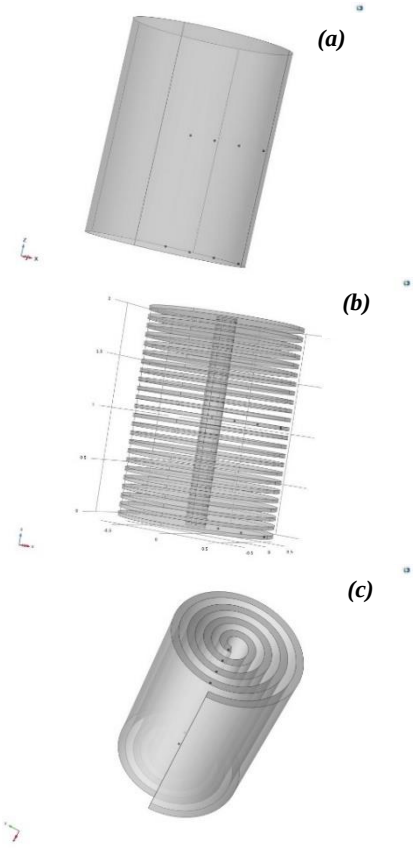

Fig. 2*: TMA designed in COMSOL in the shape of (a)bulk cylinder (b) fins-geometry and (c) spiral geometry respectively*

2. Heat transfer analysis:

For analyzing heat transfer in thermomagnetic material, we had arbitrarily chosen 3 shapes of cylinders (i.e. bulk cylinder, a fins-geometry & spiral geometry) of same basic geometric parameters (of height 2 cm and 1.5 cm diameter). On each these shapes, we have considered 8 points on which we studied temperature variation with time. These 8 points are located on 2 different planes (4 points on each plane). First 4 points were on the plane which was located at the bottom and other plane was near around the middle of the height.

2.1 Governing equation for heat transfer:

Equations (1) and (2) of heat transfer were used in these simulations for both heating and cooling processes for time dependent study.

$$\rho C_P \frac{\partial \mathrm{T}}{\partial \mathrm{t}} + \rho C_P \mathbf{u}.\nabla \mathrm{T} + \nabla.\mathbf{q} = \mathrm{Q} + \mathrm{Q_{ted}} \quad (1)$$

$$\mathbf{q} = -\mathrm{k}\nabla \mathrm{T} \quad (2)$$

Here ρ is density, C_P is specific heat at constant pressure, K is thermal conductivity ,q is heat flux, T is temperature, t is time, u is fluid velocity vector, Q is heat source, Q_{ted} is thermoelastic damping.

2.2 Model Description of heating process:

2.2.1 Model Set Up and Boundary Conditions: We built 3 models (1) a bulk cylinder of Nickel (Ni) of 1.5 cm diameter and 2 cm height (2) a Ni geometry with 24 circular fins each fin having 1.5 cm diameter and overall height 2 cm (3) a spiral Ni geometry of final diameter 1.5 cm and height 2 cm (detailed geometric specification of spiral are given below in table 1). In all these models, other geometric parameters were kept same. Nickel (Ni) domain was surrounded by Copper (Cu) domain of height 3 cm and thickness 0.1 cm. Air domain was used in between Ni domain and Cu domain as a medium. All the properties of material were taken from COMSOL Multiphysics (Version 6.1) library. Heat transfer in solids and fluids (ht) physics interface was selected. Initial Temperatures of air and Ni domain were taken as 293.15 K and initial temperature of Cu domain was taken T (i.e. T = {450 K, 550 K, 650 K}in 3 different cases) for all models and temperature variation with time was observed using point probe feature available under the node component and subnode definitions for all the 8 points.

Table 1: *All geometric specification of spiral geometry of thermomagnetic material*

S. No.	Name	Expression	Description
1	thick	0.08	Thickness of spiral (cm)
2	b1	(af-a1)/(2*pi*n1)	Spiral growth rate (cm)
3	theta_f	(af-a1)/b1	Final Angle
4	distance	(af-a1)/n1	turn to turn distance (cm)
5	b2	(gap+thick)/(2*pi)	Updated growth rate (cm)
6	theta_0	0	Initial angle
7	a1	0.075	Initial Spiral radius (cm)
8	af	0.75	final spiral radius (cm)
9	q0	0[W/m^3]	Heat flux per unit volume
10	n1	4	number of turns
11	gap	distance-thick	Gap distance (cm)

2.2.2 Mesh details and Study: For meshing these models, physics controlled Mesh was used. Element size of all these models was kept normal. Only free tetrahedral generator was used for meshing. Regarding the study, time dependent study was chosen for time interval of 100 seconds, starting from 0 to 100, taking step size of 0.1 second and temperature distribution was found for each case. (Temperature distribution on

various points of each shape for a particular case of T = 550 K is shown in figure 3)

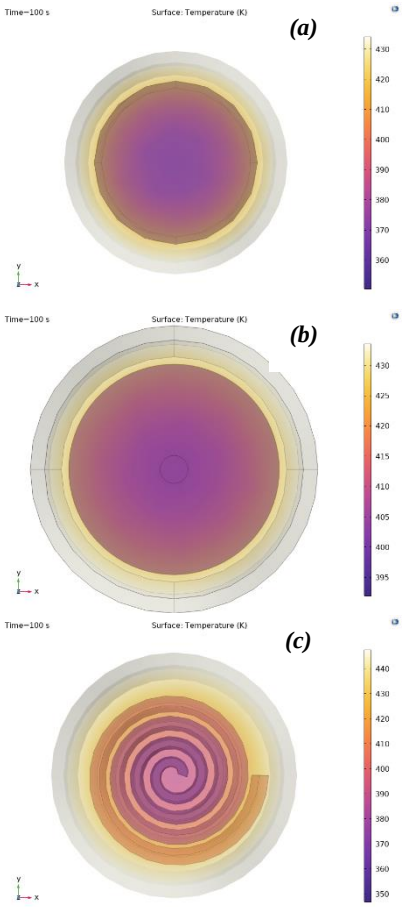

Fig 3*: Temperature distribution from top view of (a)bulk cylinder (b) fins-geometry and (c) spiral geometry*

2.3 Model Description of cooling process:

2.3.1 Model set up and Boundary Conditions:

Three geometries were developed for cooling analysis similar to the heating analysis performed previously. (1) a bulk cylinder of Nickel (Ni) alloy of 1.5 cm diameter and 2 cm height (2) a Ni alloy geometry with 24 circular fins each fin having 1.5 cm diameter and overall height 2 cm (3) a spiral Ni alloy geometry of final diameter 1.5 cm and height 2 cm (detailed geometric specification of spiral are given in table 1). In all these models, other geometric parameters were kept same. Ni alloy domain was surrounded by Copper (Cu) domain of height 3 cm and thickness 0.1 cm. Water domain was used in between Ni alloy domain and Cu domain as a medium for cooling. Volume of water domain was kept 5 times of the volume of bulk cylindrical volume. All the properties of material were taken from COMSOL Multiphysics (Version 6.1) library except properties of Ni alloy (Ni alloy properties used in the model are mentioned in the table 2). Heat transfer in solids and fluids (ht) physics interface was selected. Initial Temperatures of water and Cu domain were taken as 293.15 K and initial temperature of Ni alloy domain was taken T (i.e. T = {403.15 K ,413.15 K & 423.15 K} in 3 different cases) for all the 3 models and temperature variation with time was observed using point probe feature available under the node component and subnode definitions for all the 8 points.

Table 2: *Properties of Ni alloy*

Property	Variable	Value
Heat capacity at constant pressure	Cp	600[J/(kg*K)]
Density	rho	3000[kg/m^3]
Thermal conductivity	k_iso	18[W/(m*K)]
Electrical conductivity	sigma_iso	13.8e6[S/m]
Coefficient of thermal expansion	alpha_iso	13.4e-6[1/K]
Young's modulus	E	219e9[Pa]
Poisson's ratio	nu	0.31

2.3.2 Mesh details and Study: As we did for heating phenomena similarly for meshing these models for cooling phenomena, physics controlled Mesh was used. Element size of all trio models was kept normal. Only free tetrahedral generator was used for meshing. Regarding the study, time dependent study was chosen for time interval of 100 seconds, starting from 0 to 100, taking step size of 0.1 second and temperature distribution was found for each case. (Temperature distribution on various points of each shape for a particular case of T = 413.15 K is shown in figure 4)

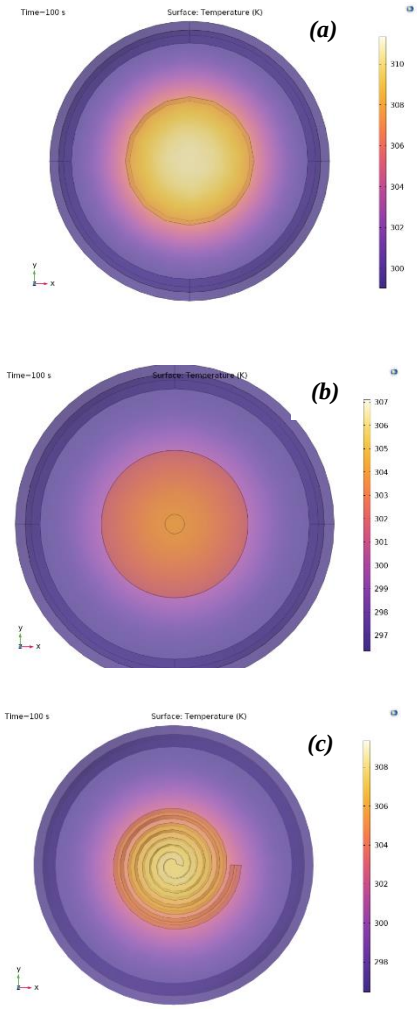

Fig 4*: Temperature distribution of (a) bulk cylinder (b) fins-geometry and (c) spiral geometry from top view*

Hence, we can infer from above description that fins-geometry is best suitable shape for TMA for faster heating and cooling process.

3. Description of axisymmetric model of TMO:

For building the model in COMSOL Multiphysics 6.1, we employed AC/DC Module, Structural Mechanics Module, Heat transfer Module and CAD Import Module.We used magnetic fields (mf), solid mechanics (solid) and heat transfer in solid and fluids (ht) physics interfaces to create an axisymmetric model.

3.1 Geometry of the model:

Initially we made a rectangle (r1) of 20 cm*28 cm for air domain. Inside that rectangle, we made second rectangle (r2) of 18 cm* 10 cm for permanent magnet (fig. 5). Then a rectangle (r4) was made of dimension 2.2 cm*8 cm for a coil. A rectangle (r5) of very small thickness of size 0.15 cm*8 cm was drawn beside the coil for quartz tube. Two rectangles (r6 & r7) of 0.15 cm*4 cm were drawn. For providing suitable contact to TMM at top and bottom, two other rectangles of size 1.15 cm*0.1cm were drawn. Two rectangles of sizes of 0.1cm *2 cm and 0.075 cm*0.0315 cm were made to generate the axis of cylinder & an array which would represent fins shaped geometry in axisymmetric form respectively.

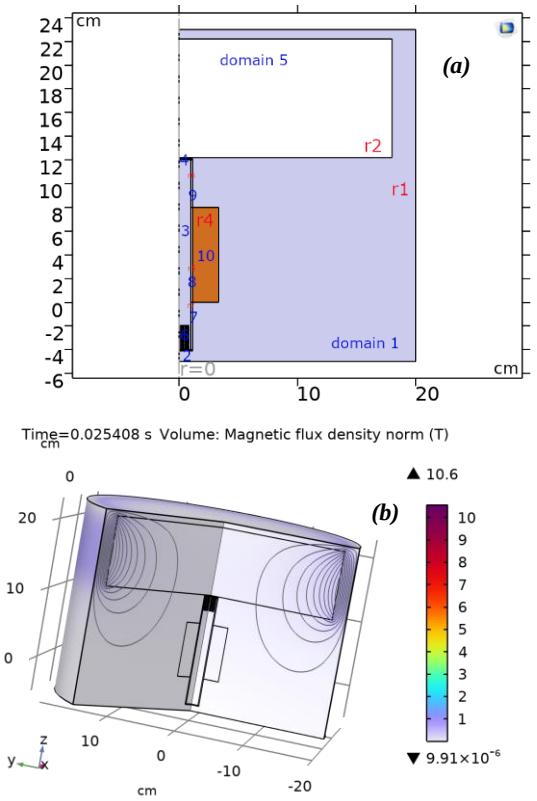

Fig: 5 (a) *Geometry of the 2D axisymmetric model* ***(b)*** *3D model representing magnetic flux density norm*

3.2 Governing Equations:

In magnetic fields (mf) interface, equation (3) of the net force F(z) acting on Ni domain was used for oscillating motion of TMM [2].

$$F(z) = F_m - F_g = ((C*\chi*(B.\nabla B))/\mu_o) - (m*g) \quad (3)$$

where F(z) was net force acting on TMM along z direction, F_m was magnetic force by permanent magnet (in upward direction), F_g was force due to gravity (in downward direction), C was volume of TMM,χ was susceptibility of TMM (temperature dependent), B was magnetic flux density of the permanent magnet, μ_o was permeability of free space, g was acceleration due to gravity and m was mass of TMM.

Equations (4 -7) which were used in the magnetic fields interface are mentioned below.

$$\nabla \times H = J \quad (4)$$

$$B = \nabla \times A \quad (5)$$

$$J = \sigma E + \sigma v \times B + J_e \quad (6)$$

$$E = -\partial A / \partial t \quad (7)$$

In above equations, H is magnetic field, J is current density, B is Magnetic flux density, A is magnetic vector potential, σ is electrical conductivity, E is electric field, v is velocity and J_e is externally generated current density.

In heat transfer in solids and fluids (ht) interface, same equations were used which we discussed in section 2.1 in solid mechanics (solid) interface, equations (8 -10) were used for time dependent study.

$$\rho \frac{\partial^2 u}{\partial t^2} = \nabla . (FS)^T + F_v \quad (8)$$

$$u(R, \Phi, Z) \rightarrow (u, 0, w)^T \quad (9)$$

$$F_v = \frac{F_{tot}}{V} \quad (10)$$

In above equations, ρ is density, F is deformation gradient, S is second Piola-Kirchhoff stress, F_v is volume force vector (force per unit volume), F_{tot} is total force and V is volume.

3.3 Material Used: For domain 1 air was taken as a medium. For permanent magnet (domain 5) BMN-52 was used. Thermomagnetic material was made of Ni (domain 6). TMM was moving up and down inside the quartz tube (domain 7,8 & 9). Coil (domain 10) and contact support (domain 2 & 4) were made of copper (fig. 5). All properties of material were taken from COMSOL Multiphysics 6.1 materials library.

3.4 Other model details:

2 contact pairs were used at upper and lower contacts of TMM with copper support & 2 domain probes were used for the domain 6 for magnetic field norm and temperature respectively. A moving mesh was used for capturing the motion of TMM. Deforming domain sub node was used for air which was deforming continuously during the motion of TMM & prescribed mesh displacement subnode was used for TMM.

In magnetic fields interface, two opposite horizontal boundaries of domain 5 were allocated as north and south pole of the magnet. Domain 10 was used as a homogenized multi turn coil. Solid mechanics interface was used only for applying force F(z) on domain 6 and using contact pairs.

In magnetic fields (mf) interface, magnetic vector potential was kept as 0 for all domains. In solid mechanics (solid) interface, the value of displacement field and structural velocity field was assigned 0 for domain 6. In heat transfer in solids and fluids (ht) interface, the initial temperature of quartz tube, air inside the tube, fins-geometry and copper support kept (domain 3,4,6,7,8 & 9) at 273.15 K. A general inward heat flux of 50000 W/ m^2 was applied at outer boundary of domain 9.

While meshing this model, we kept global size node finer. Then we used edge node for upper and lower boundaries of cylinder with fins in axisymmetric form. Then after, we used size sub node under the node edge, kept it extremely fine. For all remaining geometry, we used free triangular mesh, keeping the size extremely fine. Figure 6 represents the mesh structure near the domain 1,2 ,6 and 7.

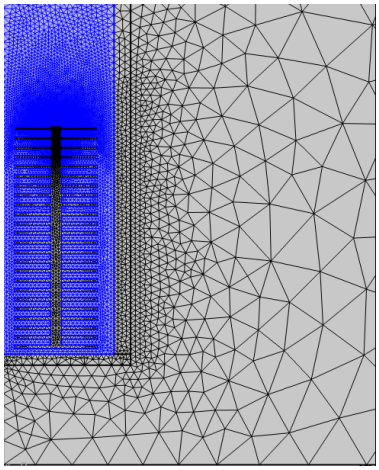

***Fig 6**: Mesh structure near the domain 6*

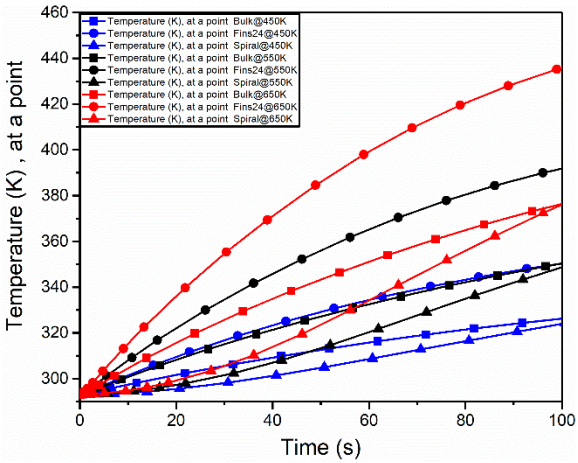

***Fig 7**: Temperature variation on a particular point (among those 8 points) with time for heating*

4. Results:

After running the simulations for all trio models for various foresaid temperatures, each point specific temperature data was arranged and its variation with respect to time was plotted in Origin Pro Software 2017 for both heating and cooling processes. These graphs represent temperature variation with time for a particular point for all three geometries. After observing these plots, we can conclude following points.

(a) Heating process was faster for Ni fins-geometry compared to other two geometries i.e. bulk cylinder and spiral geometry for all cases of temperature & at all points, hence it implied fins geometry was best suitable geometry for heating process. (Fig. 7)

(b) Cooling process was faster for fins geometry compared to other two geometries i.e. bulk cylinder and spiral geometry for all cases of temperature & at all points, hence it implies that among these geometries, fins-geometry was best suitable geometry for cooling process. (Fig. 8)

(c) During the heating process, when the initial temperature of the copper domain was 450 K, the heating rate was 53.42% faster for fins geometry with respect to bulk cylinder & 61.02% faster with respect to spiral geometry for a particular point whose temperature approaching to 320 K from 293.15 K. (Fig. 7)

(d) During the heating process, when the initial temperature of the copper domain was 550 K, the heating rate was 50.94% faster for fins geometry with respect to bulk cylinder & 68.92% faster with respect to spiral geometry for a particular point whose temperature approaching to 320 K from 293.15 K. (Fig. 7)

(e) During the heating process, when the initial temperature of the copper domain was 650 K, the heating rate was 49.6% faster for fins geometry with respect to bulk cylinder & 73.85% faster with respect to spiral geometry for a particular point whose temperature approaching to 320 K from 293.15 K. (Fig. 7)

(f) During the cooling process, when the initial temperature of the Ni alloy was 403.15 K, the cooling rate was 36.63% faster for fins geometry with respect to bulk cylinder & 38.07% faster with respect to spiral geometry for a particular point whose temperature approaching to 320 K from 403.15 K. (Fig. 8)

(g) During the cooling process, when the initial temperature of the Ni alloy was 413.15 K, the cooling rate was 29.91% faster for fins geometry with respect to bulk cylinder & 33.77% faster with respect to spiral geometry for a particular point whose temperature approaching to 320 K from 413.15 K. (Fig 8)

(h) During the cooling process, when the initial temperature of the Ni alloy was 423.15 K, the cooling rate was 27.15% faster for fins geometry with respect to bulk cylinder & 30.13% faster with respect to spiral geometry for a particular point whose temperature approaching to 320 K from 423.15 K. (Fig. 8)

Considering above mentioned points, a fins-geometry shaped TMO was developed which was discussed in section 3 in which induced voltage was 4.73 Volts while in bulk cylinder shaped geometry model, induced voltage was only 1.87 Volts. Hence, there was a hike of 152% in induced voltage after geometry optimization.

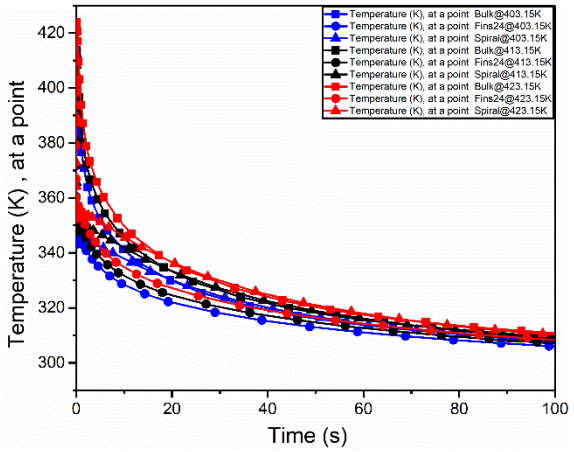

***Fig 8**: Temperature variation on a particular point (among those 8 points) with time for cooling*

5. Conclusions:

In summary, the optimization of the shape of thermomagnetic material was done in such a way that induced voltage had increased by 152% as compared to bulk cylinder shape for only upward motion of thermomagnetic alloy. This device was simple in design and can be used for waste heat utilization. Figure 8 represents induced voltage 4.73 Volts when thermomagnetic material was shaped in the form of

fins geometry while maximum induced voltage was only 1.87 Volts in case of bulk cylinder (Fig 9(a) & (b)).

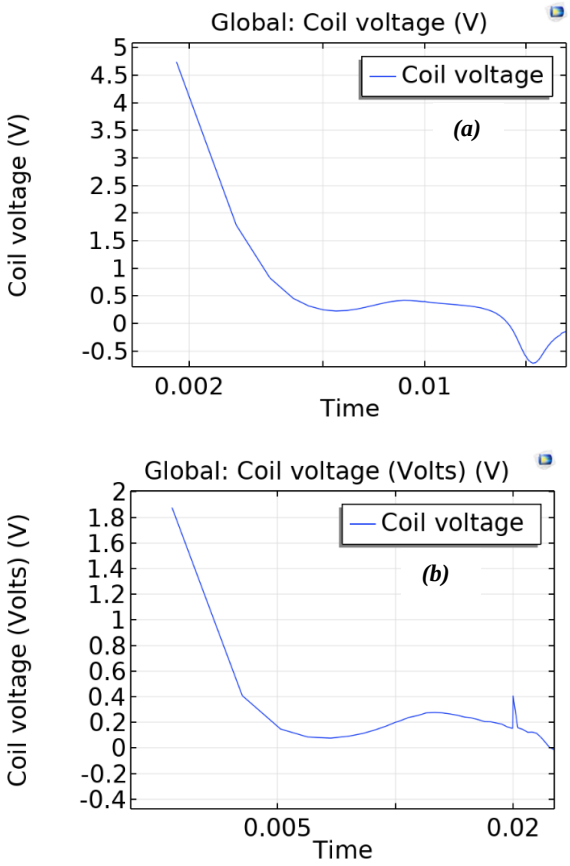

Fig:9 *(a) Induced voltage in case of fins-geometry (b) Induced voltage in case of bulk cylinder*

References

[1] K. Deepak, V. B. Varma, G. Prasanna, and R. V. Ramanujan, "Hybrid thermomagnetic oscillator for cooling and direct waste heat conversion to electricity," Appl. Energy, vol. 233–234, 2019, doi: 10.1016/j.apenergy.2018.10.057.

[2] K. Deepak, M. S. Pattanaik, and R. V. Ramanujan, "Figure of merit and improved performance of a hybrid thermomagnetic oscillator," Appl. Energy, vol. 256, 2019, doi: 10.1016/j.apenergy.2019.113917.

[3] Cesare Tozzo, "Modeling Ferromagnetic Materials in COMSOL Multiphysics", COMSOL Blog, January 23, 2018

[4] Walter Frei, "Exploiting Symmetry to Simplify Magnetic Field Modeling", COMSOL Blog, July 14, 2014

[5] Fanny Griesmer, "Quick Intro to Permanent Magnet Modeling", COMSOL Blog, June 21, 2013

[6] Mark Fowler, "Computing Voltages Produced by Electromagnetic Induction", COMSOL Blog, June 17, 2014

[7] Nirmal Paudel, "Part 1: How to Model a Linear Electromagnetic Plunger", COMSOL Blog, June 7, 2016

[8] Rachel Keatley, "Analyzing LED Bulb Designs with Heat Transfer Simulation", COMSOL Blog, July 22, 2021

[9] Bridget Paulus, "Designing Heating Circuits with Multiphysics Simulation", COMSOL Blog, February 12, 2019

[10] COMSOL Multiphysics Reference Manual (Version 5.5), 1998–2019 COMSOL.